Investigation of seismic performance of cable-stayed bridges with different connections

J.L. Liu[1], H. Li[2] and J.P. Ou[2,3]

[1] *PhD Candidate, School of Civil Engineering, Harbin Institute of Technology, Harbin 150090, China*
[2] *Professor, School of Civil Engineering, Harbin Institute of Technology, Harbin 150090, China*
. [3] *Professor, School of Civil Engineering and Hydraulic Engineering, Dalian University of Technology, Dalian, 116024, China*
Email: liujinlong@hit.edu.cn

ABSTRACT :
In this paper, the seismic behaviors of three cable-stayed bridges with different structural systems include Rigid System (RS), Floating System (FS) and Passive Energy Dissipation System (PEDS) are studied. The result shows that the seismic behaviors of these bridges are different largely even under the same earthquake. These behaviors include the displacement and force response of the main components in three cable-strayed bridges which are compared in detail as follows. Based on damage analysis of the towers, failure modes of the three different systems were concluded. For RS, the bottom of the middle tower is a vulnerable region, this means the failure is focused here and plastic hinge formed under earthquake. The FS is damaged most severely, in which the edge tower has a largest damage index. While the seismic responses of PEDS are decreased largely compared to FS due to the employ of viscous dampers and the damage indices for all towers are cut down, remarkably the dissimilarity of damage condition between middle tower and edge tower can be adjusted by changing the damping coefficient of the viscous material, the damage of middle tower can be identical to that of edge tower if the damping coefficient is rational.

KEYWORDS:
failure mode, structural systems, rigid system, floating system, passive energy dissipation system

1. INTRODUCTION

For cable-stayed bridges, a very large step forward took place in 1990s, when cable-stayed bridges entered the domain of very long spans. At this time, the research on the seismic performance of cable-stayed bridges progressed rapidly, as summarized below.
Following the 1988 Saguenay earthquake, one anchorage plate connecting the steel box girders to one abutment of the cable-stayed bridge near Jonquière Québec was failed. The static and dynamic analysis were carried out by Filiatrault et al[1,2], the results showed that the anchorage plates were subjected to high stress concentrations under dead load, and the stress increments induced by the earthquake led to the failure. Adeli and Zhang[4] studied the full nonlinear performance of composite girder cable-stayed bridge with fan, semi-fan and harp types in 1995. Based on the Jindo Bridge located in South Korea, Schemmanni and Smith[6,7] studied how the non-linear behavior and the participation of highly coupled and high-order vibration modes in the overall dynamic response affected the effectiveness of active control schemes in 1998. Ren and Obata[5] investigated the elastic-plastic seismic behavior of long span cable-stayed steel bridges through the plane finite-element model in 1999. In 2000, Caetano et al[8,9] studied the dynamic interaction between the cables and the deck/towers system of cable-stayed bridges in seismic excitation. In 2005, McDaniel and Seible[12] studied the influence of inelastic tower links on the seismic response of cable supported bridges. Based on the benchmark cable-stayed bridge model, much works for the seismic control of cable-stayed bridges have been done.
For long span cable-stayed bridges, the floating system is a suitable choice but not the rigid system for the influence of temperature stress. However the longitudinal displacement response of this system is very large usually, some measures must be done to decrease the displacement and fixing dampers is a good method. But comprehension for the performance of these different structure systems is even scarce. In this paper, the performances of three cable-stayed bridges with different connections under ground motions were studied, and the failure modes of these different system bridges are achieved based on damage analysis of the towers.

2. MODELING OF CABLE-STAYED BRIDGES

2.1. Description of bridges

The Shandong Binzhou Yellow River Highway Bridge is employed for this study, as shown in Figure 1. The main bridge has a total length of 768 m consisting of two spans of 300 m each and two side spans of 84 m each. The bridge contains three towers and each of them consists of two pre-stressed concrete (PC) legs. The middle tower has a height of 125.28 m, while the other two edge towers are both 75.78 m high. The deck is composed of two PC box girders and PC slab, which has a total width of 32.8 m. Figure 3(a) shows the initial cross-section shape of the box girder. For conveniently establishing the finite element model in OpenSees, the triangle cross-section shape is substituted by a rectangle shape through equivalent stiffness principle, as shown in Figure 3(b). The total 200 stay cables are arranged within a double-plane system symmetrically and the layout of the cables in half plane is displayed in Figure 2.

Figure 1 Elevation view of the bridge

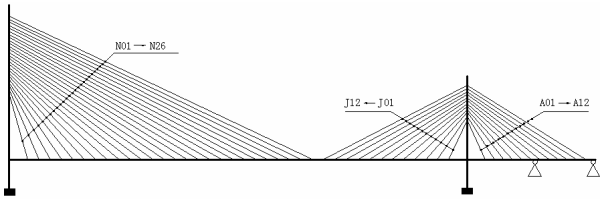

Figure 2 Layout of the cable in half plane

For this bridge, the middle tower is rigidly connected with two-side girders, while the two edge towers and other piers only supply a vertical sustainment for the girders. So this bridge is called as 'Rigid System (RS)', and Figure 4(a) shows the schematic plan of this system. Considering that the connection configuration of the tower with the girders is critical to the seismic performance of a bridge, following two modified configurations are considered in this study: (i) joint of the middle tower and the girder with a single vertical support, just like the edge towers and the other components maintained, thus the Rigid System is converted to 'Floating System (FS)', as shown in Figure 4(b); and (ii) damper elements are employed which located between the middle tower and the girders, and oriented to apply forces longitudinally which system is called as the 'Passive Energy Dissipation System (PEDS)', as shown in Figure 4 (c).

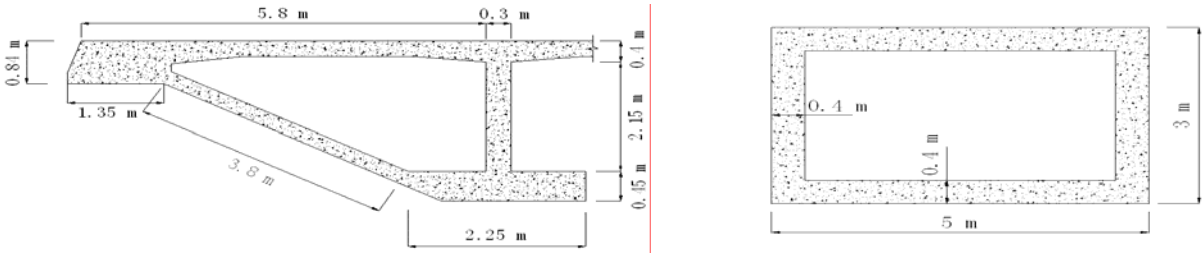

(a) Original cross-section (b) Equivalent cross-section

Figure 3 The cross-section of the girder

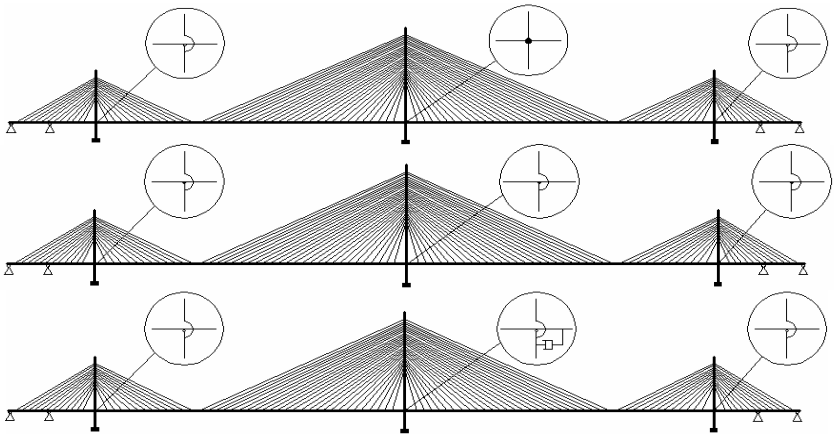

(a) RS

(b) FS

(c) PEDS

Figure 4 Configurations of different bridge systems

2.2. Material properties

The girder, tower, deck, stay cable, and transverse beams are the main components of the bridge. Most of them are pre-stressed concrete members except the cable which is comprised of 7 mm high-strength wires and is protected by a high-density polyethylene sheath.

The uniaxial Kent-Scott-Park model with degraded linear unloading/reloading stiffness is employed to modeling the strain-stress relationship of the concrete which neglects the tensile strength of the concrete, as shown in Figure 5(a), and the model parameters are list in Table 1. A bilinear model is employed to denote the strain-stress relationship of the reinforced bars embedded in girders, towers, beams and deck, as shown in Figure 5(b) and Table 1. The high strength steel wire used in stay cable is simulated by pre-stressed elastic constitutive model (Young's modulus E=210 GPa) with a tensile strength of 1800 MPa. The damping coefficient $C = 10{,}000\text{kN}/(\text{ms}^{-1})$ and velocity exponent $\alpha = 0.4$ of liquid viscous material are used.

Table 1 Material properties of concrete and common steel

Confined concrete	f_c (MPa)	f_{cu} (MPa)	ε_c	ε_{cu}
	49.7	37.3	0.004	0.02
Common concrete	f_c (MPa)	f_{cu} (MPa)	ε_c	ε_{cu}
	35.5	0	0.002	0.006
Common Steel	E (MPa)	f_y (MPa)	b	
	200000.0	335.0	0.01	

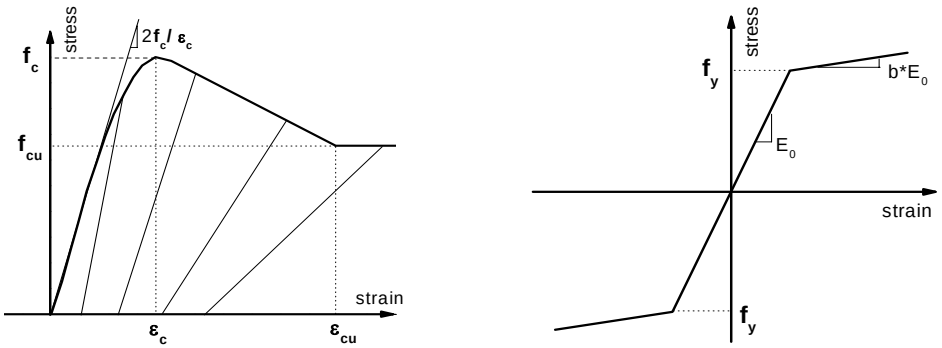

(a) Concrete material model (b) Common steel material model

Figure 5 Material constitutive models

Table 3 Components of ground motions

Earthquake	PGA of Each Component			Earthquake	PGA of Each Component		
Chi-Chi/ TCU052	N	V	W	Imperial Valley/ El Centro	S00E	S90W	VERT
	0.419g	0.241g	0.348g		0.34g	0.21g	0.21g

2.3. Finite-element model

The three dimensional finite element models for this cable-stayed bridge are built in OpenSees. The towers, the girders and the transversal beams are all simulated by nonlinear beam-column elements with fiber sections. The stay cables are modeled with truss elements which connect the tower and the girder. Remarkably, the slab is simulated by nonlinear beam-column elements in two directions.

Constraints are applied to restrict the girder (deck) from moving laterally at towers and piers for all systems. In longitudinal direction, the girder is unrestricted with side towers and piers for all systems, while discrepancy is presented at the connection of girder with middle tower for different systems. These differences are: (i) for RS, the girder element and middle tower element share the same node at the intersection, thus they are rigidly connected; (ii) for FS, there are two points at the intersection, one belongs to middle tower, while the other belongs to the girder. Although the two points have the same coordinate, they have no restriction each other. Thus the tower element and girder element can shift freely. (iii) for PEDS, 2 damper elements are employed which located between the middle tower and the girders, and oriented to apply forces longitudinally.

3. INPUT GROUND MOTIONS

To evaluate the effects of different strong ground motions on the seismic response of long span cable-stayed bridges, two earthquake records are used in this analysis. They are all downloaded from PEER strong motion database. The detailed information of the ground motion recorder is listed in Table 3. Remarkably the TCU052 record is a typical near-fault ground motion which has a larger velocity pulse compared with El Centro record. The bridge longitudinal direction refers to the N component of TCU052 record and the S00E component of El Centro array, while the vertical direction refers to the V component of TCU052 record and the VERT component of El Centro array.

4. SEISMIC BEHAVIOURS OF THE MODELS

Nonlinear time-history responses of the three bridge models under two earthquake records are simulated. The two strong ground motion records are input along the bridge longitudinal direction combined with vertical direction after static computation under dead load. The components of the ground motion records are input in the corresponding directions as mentioned above, and the peak accelerations of the ground motions are adjusted to be consistent. The peak accelerations of longitudinal component are adjusted to 0.2g while that in the vertical direction are adjusted to 0.13g. Material and geometric nonlinearities are considered in the analysis.

4.1 Displacements response of towers

Figure 6 shows the longitudinal displacements time-history response at the top of middle towers under El Centro and TCU052 record. From the figure we can get that, the FS has the largest longitudinal displacement response, the RS has the minimum response, while the response of PEDS is medium under both ground motion. Although under El Centro ground motion the maximum response of FS is as much as that of the PEDS, the courses of the time-history of them have much difference as shown in figure 6(a), this indicate the response of FS is composed of large vibration amplitudes with long period which can cause more destruction to cable-stayed bridges. Contrast figure 6(a) and 6(b), we can find that under TCU052 ground motion the displacements response are much larger than that under El Centro record, especially for FS, this means that near fault earthquake with large velocity pulse can cause more displacement response to long span cable-stayed bridges, and this effect is more remarkable for FS.

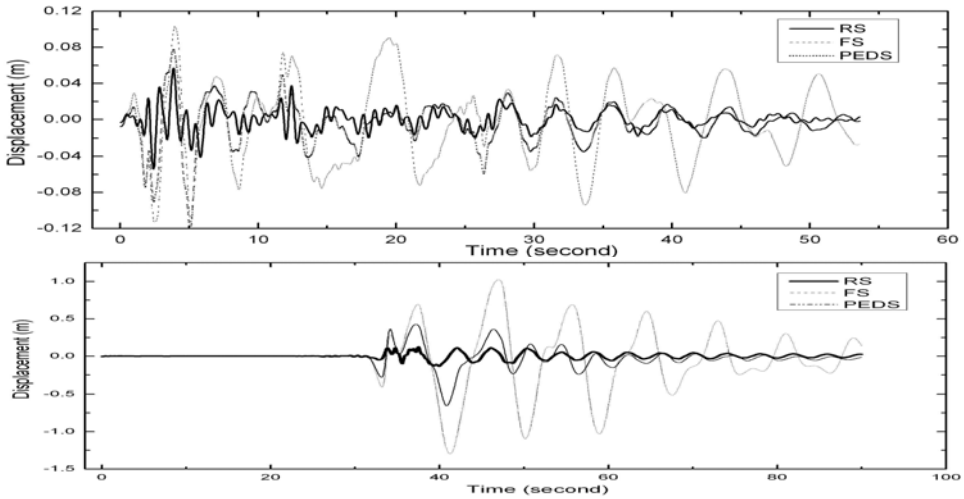

Fig 6 Top displacement time history of middle tower (a) El Centro record (b) TCU052 record

Figure 7 gives the top displacement time history of left tower for three systems, just like middle tower, the FS has the largest displacement responses among the three systems, the RS has the minimum one, while the response of PEDS is medium. The left tower has an initial displacement due to the pre-stressing force in the cables, and the tower vibrates around the initial position under the excitation of ground motions. Compared with

Figure 6 we can find that the top displacement left tower is even larger than that of middle tower, this will cause more flexure to left tower because left tower is shorter than middle tower.

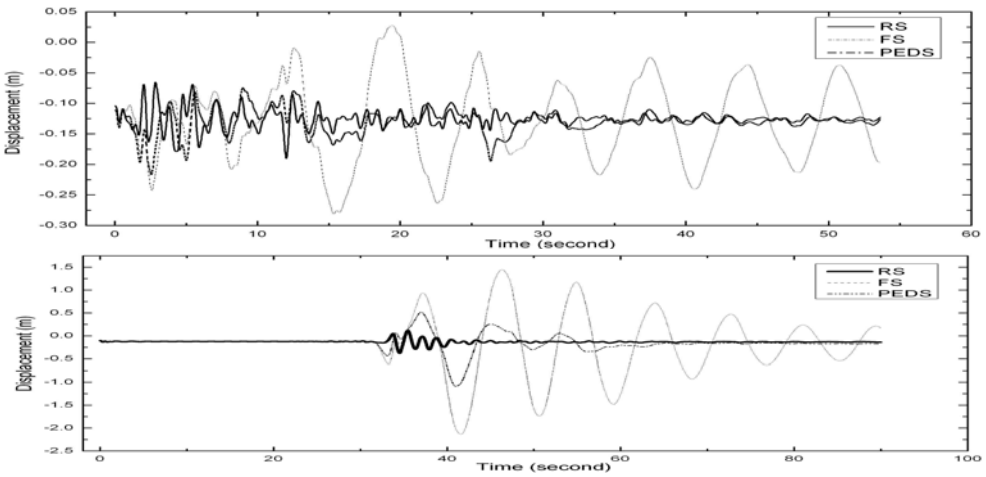

(a)

(b)

Fig 7 Top displacement time history of left tower (a) El Centro record; (b) TCU052 record

4.2 Girder displacement response

Because the girder and deck are integrated, the displacements of them are coherent. The longitudinal displacement response of the girder at the joint with middle tower of each system is shown in figure 8. The longitudinal girder displacement of RS is small, even under TCU052 earthquake, the maximum displacement is only 0.125 m. But the reaction of FS is very large, and the maximum displacement response of FS is increased to 1.6 m under TCU052 record. Contrast to displacement of tower, the longitudinal displacement of girder can cause more destruction to the bridge, for example the damage of support abutment, the collision of the girder, and so on. When the dampers are fixed between the girder and middle tower, the longitudinal displacement of the girder is decreased sharply. Not only the maximum response is reduced, the vibration is attenuated quickly, as shown in figure 8, this can protect the bridge from being destroyed by strong ground motions.

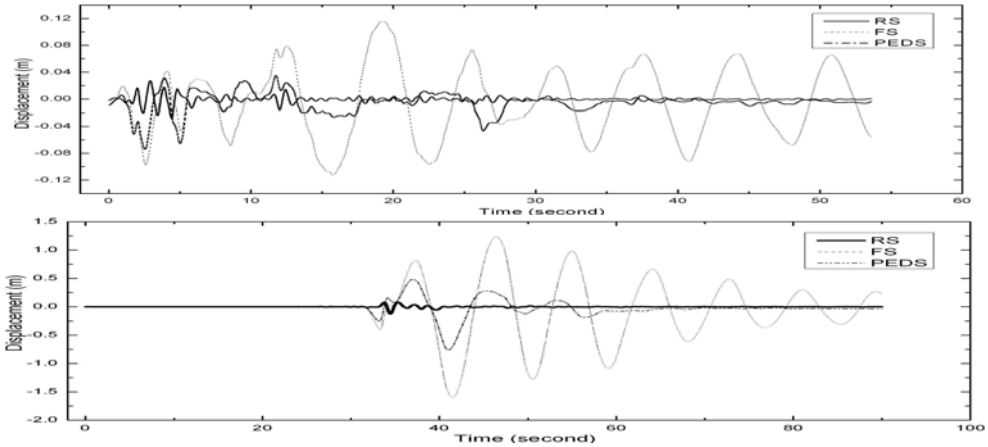

(a)

(b)

Fig 8 Girder displacement time history (a) Under El Centro record; (b) Under TCU052 record

4.3 Force vibration in N26 cable

The force vibrations of N26 cable are shown in figure 9. Under El Centro earthquake, the force vibrations are very little for all systems. The FS has the maximum response, while the maximum incremental force is only about 7% of the initial force in cable. But under TCU052 earthquake, the vibration of the force become drastic, especially for FS, the peak value of the incremental cable force is come up to 8.29×10^6 N which is about 29.5% of the initial force in cable. When the dampers are incorporated, the vibration decreased to near the response of RS, as shown in figure 9. This means the dampers are effective to reduce the vibration of cables.

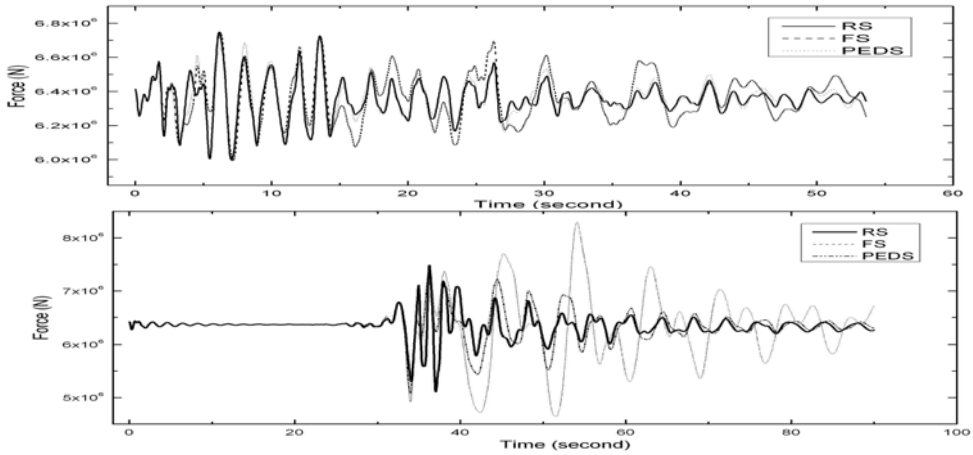

Fig 9 Force time history in N26 cable (a) Under El Centro record; (b) Under TCU052 record

4.4 Envelop of the response

Figure 10 shows the peak tower bending moments in longitudinal direction as a function of the height of middle tower for three systems under two excitations. From the figure we can get that the RS has the largest bending moment at the bottom of middle tower. Because the girder and the tower are rigid connected in RS, this leads to the peak bending moment below the girder increase rapidly, and the envelop curve has an abruptly change at the intersection between the girder and middle tower; above this joint, the maximum bending moment is steady as far as the intersection between N01 cable and middle tower; then the envelop value of the bending moment decrease with the height of tower to zero at top. For FS and PEDS, the variation of the envelop value of the bending moment along the tower height is harmonious, as shown in figure 10, this distribution of bending moment is help for the tower which has a continuously variable crossing-section to resist the bending moment. From the two figure, we can find that the envelop values of the bending moments under TCU052 earthquake is more than that under El Centro earthquake.

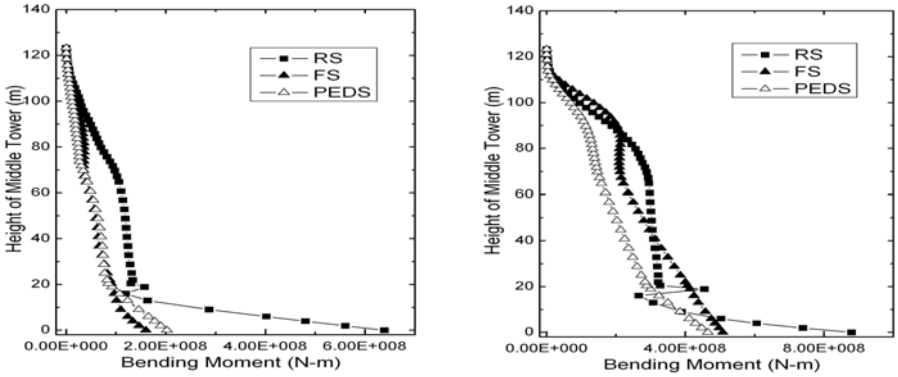

(a) Under El Centro array (b) Under TCU052 array

Fig 10 Envelop of the bending moment along the height of middle tower

5. SEISMIC DAMAGE ANALYSIS OF TOWERS

Under strong ground motions, the cable-stayed bridges will develop to plastic stage with low cycle fatigue. In order to reflect the influence of plastic development and low cycle fatigue to the seismic damage of cable-stayed bridge, Park and Ang[13] seismic damage model for the RC structure is used which consider the maximum displacement response and repeated cyclic loading effect to analyze the seismic damage of the bridge under TCU052 earthquake. The damage index is proposed by Eqn.5.1:

$$D = \frac{x_m}{x_{cu}} + \beta \frac{E_{hs}}{F_y x_{cu}} \tag{5.1}$$

In which D = damage index; x_{cu} = ultimate deformation under monotonic loading; F_y = calculated yield strength; x_m = maximum deformation under earthquake; E_{hs} = cumulative absorbed hysteretic energy; β = energy dissipation factor which can be calculate by Eqn.5.2:

$$\beta = (-0.447 + 0.073\lambda + 0.24n_0 + 0.314\rho_t)0.7^{100\rho_w} \tag{5.2}$$

In which λ = shear span ratio (replaced by 1.7 if λ < 1.7); n_0 = normalized axial stress (replaced by 0.2 if n_0 < 0.2), ρ_w = confinement ratio, ρ_t = longitudinal steel ratio as a percentage (replaced by 0.75% if ρ_t < 0.75%).

For the modeling cable-stayed bridges, the components such as girders, transverse beams, cables and decks are difficult to develop plastic. So only the towers need to be analyzed. This paper selects left tower and middle tower as the analysis objects. The restoring model parameters of these legs obtained form nonlinear static analysis, and the maximum displacements of towers, the cumulative absorbed hysteretic energy and the damage indices under TCU052 earthquake are given in table 4.

6. FAILURE MODES BASED ON DAMAGE ANALYSIS

From seismic damage analysis of towers together with the response of the bridge under earthquake, the seismic failure modes of cable-stayed bridges for different structural systems are concluded.

(1) For RS, the damage is concentrated at middle tower which has a damage index of 0.54 as shown in table 4, and this indicates the middle tower is in moderate damage condition[13], but the left tower is only slightly damaged with a damage index of 0.17. Thus we can find that the seismic damage of RS is mainly focus on middle tower which has the largest bending moment at the bottom among the three systems as shown in figure 10, and the plastic hinge is formed at the bottom section. Since the tower has a rigid intersection point with the girder, the peak bending moment of the tower below the girder increase rapidly, this means a vulnerable region is formed and larger flexural effects are suffered here.

Table 4 Dissipated energy and damage indices

		RS	FS	PEDS (C=1e4kN-s/m)	PEDS (C=2e4kN-s/m)
Middle tower	Maximum displacement (m)	0.11	1.30	0.65	0.51
	Dissipative energy (N-m)	1.25×10^7	9.33×10^6	0	0
	Damage indexes	0.54	0.59	0.31	0.16
Left tower	Maximum displacement (m)	0.28	2.03	0.97	0.50
	Dissipative energy (N-m)	1.17×10^6	1.89×10^7	2.37×10^6	0
	Damage indexes	0.17	1.77	0.50	0.19

(2) For FS, the damage is the severest one. The damage indices of left tower and middle tower are increased to 1.77 and 0.59 respectively as shown in table 9, this indicates the service ability of left tower is completely lost even the tower will be broken down and the middle tower is in moderate damage condition[13]. So we can conclude that the failure of FS is firstly from edge tower and middle tower is secondary.

(3) For PEDS, the damage is greatly improved compared to FS because the usage of liquid viscous dampers. The damage indices of left tower and middle tower are decreased to 0.50 and 0.31 respectively as shown in table 9. This means the dampers are very beneficial for the cable-stayed bridges to resist the destruction from earthquake for FS. However there are even some discrepancy between the damage condition of left tower and middle tower, the left tower is damaged more seriously than middle tower like the FS. In order to eliminate this difference, we increase the damping coefficient of the liquid viscous material from $C = 1\times10^4\, kN/(ms^{-1})$ to $C = 2\times10^4\, kN/(ms^{-1})$, and then the indices of the two tower are calculated, they are 0.16 and 0.19 for left tower and middle tower respectively. We can find not only the damage state is improved, the dissimilarity of the damage indices between middle tower and left tower are eliminated largely, in other words, the distribution of seismic action between edge tower and middle are more harmoniously; thus they can resist the seismic load in step and the failure load capacity under earthquake is enhanced.

7. CONCLUSIONS

Several observations can be made from the results of the preceding analysis:
The behaviors of long span cable-stayed bridge under various earthquakes with the same PGA will have much difference. It depends highly on the characteristics of earthquake records. Under near fault earthquake records with large velocity pulse, the response of the bridge will increase largely, especially for the FS. So the earthquake record with the largest PGA value does not necessarily induce the maximum responses.
There is much diversity of the seismic performance among three systems.
Although there are some differences between the structural systems of the cable-stayed bridges, the seismic damages are mostly concentrated at towers while the other components are difficult to failure for all systems.
Based on damage analysis of towers, failure modes of the three cable-stayed bridges are concluded. For RS, the damage is concentrated at middle tower with a vulnerable region below the girder. The damage of FS is most seriously, while the failure is from the edge tower and then the middle tower. For PEDS the damage condition is improved largely compared to FS due to the existence of dampers. The PEDS can make full use of the advantages of RS and FS and avoid the shortcomings of them, whose force response is reduced contrast to RS, simultaneity, the displacement response is decreased compared with FS; thus the performance of PEDS is more dominant than RS and FS. Moreover the discrepancy of the damage between middle tower and left tower can be eliminated via adjusting the damping coefficient of the liquid viscous material, and this can enhance the ability of the cable-stayed bridge to resist the seismic action.

ACKNOWLEDGE

This study is financially supported by the Ministry of Science and Technology with Grant No. 2007CB714204, 2007CB714205 and 2006BAJ03B06.

REFERENCES

1. Filiatrault A, Tinawi R, Massicotte B. (1993). Damage to cable-stayed bridge during 1988 saguenay earthquake. I: pseudostatic analysis. *Journal of Structural Engineering (ASCE)* **119(5)**:1432-1449.
2. Filiatrault A, Tinawi R, Massicotte B. (1993). Damage to cable-stayed bridge during 1988 saguenay earthquake. Ⅱ: dynamic analysis. *Journal of Structural Engineering (ASCE)* 1993 **119(5)**:1450-1463.
3. Virlogeux M. (1999). Recent evolution of cable-stayed bridges. *Engineering Structures* **21(8)**:737-755
4. Adeli H, Zhang J. (1995). Fully nonlinear analysis of composite girder cable-stayed bridges. *Computation & Structures* **54(2)**:267-277.
5. Ren WX, Obata M. (1999). Elastic-Plastic Seismic Behavior of Long Span Cable-Stayed Bridges. *Journal of Bridge Engineering* **4(3)**:194-203.
6. Schemmann AG, Smith HA. (1998). Vibration control of cable-stayed bridges-Part 1: modeling issues. *Earthquake Engineering and Structural Dynamics* **27(8)**:811-842.
7. Schemmann AG, Smith HA. (1998). Vibration control of cable-stayed bridges-Part 2: control analyses. *Earthquake Engineering and Structural Dynamics* **27(8)**:825-843.
8. Caetano E, Cunha1 A, Taylor CA. (2000). Investigation of dynamic cable-deck interaction in a physical model of a cable-stayed bridge. Part I: modal analysis. *Earthquake Engineering and Structural Dynamics* **29(4)**:481-498.
9. Caetano E, Cunha1 A, Taylor CA. (2000). Investigation of dynamic cable-deck interaction in a physical model of a cable-stayed bridge. Part II: seismic response. *Earthquake Engineering and Structural Dynamics* **29(4)**:499-521.
10. Gentile C, Cabrera FM. (2004). Dynamic performance of twin curved cable-stayed bridges. *Earthquake Engineering and Structural Dynamics* **33(1)**:15-34.
11. Dyke SJ, Caicedo JM, Turan G, Bergman LA, Hague S. (2003). Phase I benchmark control problem for seismic response of cable-stayed bridges. *Journal of Structural Engineering (ASCE)* **129(7)**:1450-1463.
12. McDaniel CC, Seible F. (2005). Influence of Inelastic Tower Links on Cable-Supported Bridge Response. *Journal of Bridge Engineering (ASCE)* **10(3)**:272-280.
13. Park YJ, Ang AH-S. (1985). Mechanistic seismic damage model for reinforced concrete. Journal of *Structural Engineering (ASCE)* **111(4)**:722-739.